GEOPHYSICAL RESEARCH LETTERS, VOL. 27, NO. 16, PAGES 2369-2372, AUGUST 15, 2000

Seismic heterogeneity in the upper crust near the 1991 eruption site on the East Pacific Rise, 9°50'N

T. Tian,[1,5] William S. D. Wilcock,[2] Douglas R. Toomey,[3] and Robert S. Detrick[4]

Abstract. We report the results of a small-aperture upper-crustal tomography experiment conducted on the East Pacific Rise near 9°50'N, the site of a volcanic eruption in 1991. The experiment geometry comprised 3 ocean bottom seismometers and 491 airgun shots fired in a 16 x 16 km^2 area. Two- and three-dimensional inversions indicate that the average upper crustal velocities, both on and off axis, increase by ~0.2 km/s north of 9°52'N. This location coincides with the northern limit of the 1991 eruption and of vigorous hydrothermalism. Our data can be explained by a 100 m southward increase in layer 2A thickness. On axis, previous work indicates that layer 2A thickness does not vary in this region. We infer that the sheeted dikes above the axial magma chamber are thermally segmented with the dike layer south of 9°52'N being on average at least 300°C warmer than to the north. Off axis, layer 2A may be thicker south of 9°52'N if a higher proportion of eruptions flow off axis.

1. Introduction

The EPR between 9° and 10°N is a well-studied section of a fast-spreading ridge, with the region near 9°50'N receiving particular attention since the detection in 1991 of an eruption along a fourth-order segment extending from 9°45'N to 9°51.5'N [*Haymon et al.*, 1993]. The eruption site lies on the shallowest and most inflated portion of this part of EPR and overlies the hypothesized position of a mantle diapir [e.g., *Barth and Mutter*, 1996]. Since the 9°45'-9°51.5'N segment is known to be magmatically and hydrothermally active, it can be inferred that this region has a high-magma budget on both short timescales of ~10-100 years and longer timescales of at least 10^5 years [e.g., *Scheirer and Macdonald*, 1993].

In this paper, we present the results of a small aperture seismic tomography experiment near 9°50'N to image upper crustal structure. The results show that the upper-crustal structure changes near the fourth-order segment boundary at 9°52'N both on-axis and out to ages of 10^5 years, the maximum age sampled by the experiment.

2. Experiment and Methods

The 1997 UNDERSHOOT experiment [*Toomey et al.*, 1998] was a segment-scale seismic experiment with the primary objective of imaging the lower crust and the crust-mantle boundary (the Moho) in order to constrain along-axis variations in melt supply beneath a fast spreading ridge. As a minor component of the UNDERSHOOT experiment, we conducted a tomographic experiment near 9°50'N to image upper crustal structure. The experiment (Figure 1) comprised three ocean bottom seismometers (OBSs) and 491 airgun shots. One OBS was deployed on the ridge axis at 9°50.5'N and the other two were located 6 km to either side of the rise. The seismic source was the 20-gun array of the *R/V Maurice Ewing* with a total volume of 139 liters (8,500 cubic inches). The shots were spaced 300 m apart along eight 15-km-long shot lines that were oriented perpendicular to the ridge axis and separated by about 2 km. This experiment geometry yields good ray sampling in the upper crust down to about 2 km depth. Our data set for this study comprised travel time picks for over 800 P-wave first arrivals that were identified by visual methods with an estimated uncertainty of less than 10 ms. We have excluded travel times for paths that pass below the magma chamber [*Wilcock et al.*, 1995].

We have applied the tomographic technique of *Toomey et al.* [1994] which employs graph theory [*Moser*, 1991] to estimate ray paths and travel times and includes the effects of bathymetry. For this study, the slowness model for the forward problem is defined on a 200 m grid in a $16 \times 16 \times 2$ km^3 volume which is rotated to the trend of the ridge axis and en-

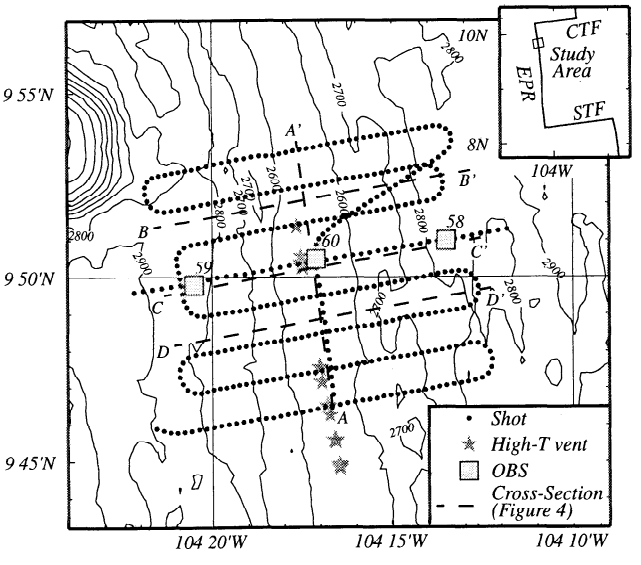

Figure 1. Bathymetry map contoured at 100 m showing the configuration of the seismic tomography experiment and the location of high-temperature vent sites [*Haymon et al.*, 1991]. Dashed lines show the locations of the four vertical cross-sections shown in Figure 4. The inset figure shows the location of the experiment area on the East Pacific Rise between the Clipperton (CTF) and Siqueiros (STF) transform faults.

[1]Geophysics Program, University of Washington, Seattle
[2]School of Oceanography, University of Washington, Seattle
[3]Department of Geological Sciences, University of Oregon, Eugene
[4]Department of Geology and Geophysics, Woods Hole Oceanographic Institution, Woods Hole, Massachusetts
[5]Now at Department of Electrical Engineering, Arizona State University, Tempe

Paper number 1999GL011191.
0094-8276/00/1999GL011191$05.00

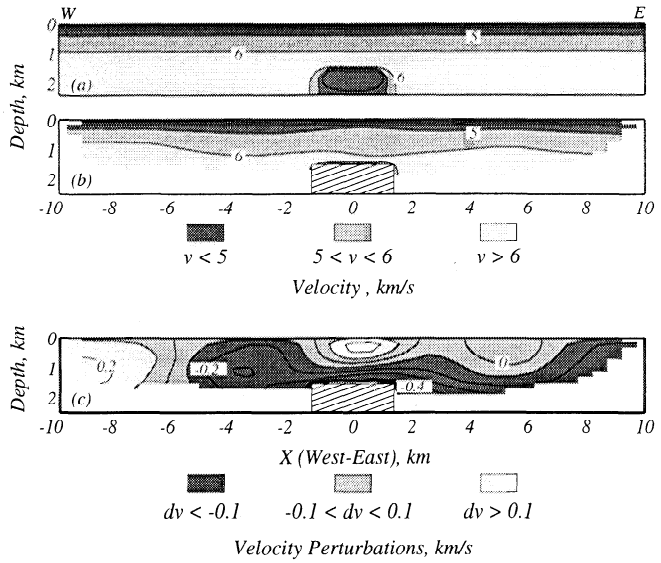

Figure 2. Results of a two dimensional inversion for the across axis velocity structure. (a) The starting velocity model. (b) The final velocity model. Regions that are unsampled by ray paths are blanked out and the hatched area shows the location of the AMC anomaly included in the starting model. (c) The velocity perturbation model (final model minus starting model).

closes all of the shots and receivers. The nonlinear inverse method solves for slowness perturbations by minimizing a functional that includes travel time residuals and horizontal and vertical smoothing constraints. We inverted for both two- and three-dimensional perturbation models with horizontal and vertical grid spacings of 200 m and 500 m, respectively. For each inversion, we obtained solutions with a variety of smoothing parameters and we repeated inversions with different starting models. All the results reported here are insensitive to the starting model and show similar features for a wide range of smoothing parameters.

3. Results

The starting model for a two-dimensional inversion (Figure 2a) was obtained by combining a one-dimensional velocity-depth profile determined from our off-axis travel time data with the axial magma chamber (AMC) velocity structure obtained by *Vera et al.* [1990] at 9°30'N. The RMS travel time residual for our preferred two-dimensional solution (Figure 2b-c) is 23 ms compared to 35 ms for the best fitting one-dimensional model, a variance reduction of 57%.

The inversion results reveal three features that are also observed in tomographic models for the 9°30'N region [*Toomey et al.*, 1990, 1994]. First, there is an axial high-velocity anomaly at depths less than 1 km. This feature is generally accepted as being due to thinning of the extrusive layer 2A on the ridge axis [*Toomey et al.*, 1990; *Harding et al.*, 1993; *Christeson et al.*, 1994]. At 9°50'N this feature is markedly less pronounced than at 9°30'N. The maximum anomaly in Figure 2c is only 0.2 km/s compared to average maximum values of about 0.5 km/s in a three dimensional inversion at 9°30'N [*Toomey et al.*, 1994]. Second, there is a low velocity anomaly above the AMC whose magnitude increases with depth. *Toomey et al.* [1994] interpreted a similar feature at 9°30'N in terms of elevated temperatures within the sheeted dike complex above the AMC. Third, the cross-axis velocity structure is asymmetric, with the west slower than the east. Near 9°30'N this asymmetry is attributed to higher levels of off-axis volcanism producing a thicker layer 2A on the west flank [*Harding et al.*, 1993; *Christeson et al.*, 1994; *Toomey et al.*, 1994].

The travel time residuals for the two-dimensional inversion vary systematically along-axis (Figure 3). The most prominent change occurs in the northern part of the experiment near 9°52'N (y = 3 km). Here, the mean residuals calculated for each across-axis shot line decrease by about 30-40 ms to the north, a result that suggests slower seismic velocities to the south. This change coincides closely with a fourth-order segment boundary at 9°51.5'N [*Haymon et al.*, 1991] that marks the northern limit of the 1991 eruption [*Haymon et al.*, 1993].

Although our experiment is not ideal for three-dimensional imaging due to the linear distribution of recording sites, the data clearly requires along axis velocity variations. Our preferred three-dimensional solution (Figure 4) has an RMS residual of 18 ms compared to 23 ms for the two-dimensional inversion, a variance reduction of 39%. Seismic velocities are substantially higher in the northern half of the model. The near-surface axial high-velocity anomaly is barely present in the south but has an amplitude of up to 0.3 km/s in the north. The velocities in the low-velocity anomaly above the AMC increase northward by a similar amount. There are also substantial increases in velocity off-axis, particularly on the western flank.

To analyze our data for the effects of crack-induced anisotropy, we calculated mean residuals for ray paths falling in 20° azimuth bins for the three-dimensional inversion (Figure 5). The most positive residuals (slowest arrivals) are generally observed for rays travelling across axis. For shots to the south, the residuals show little variation with azimuth while

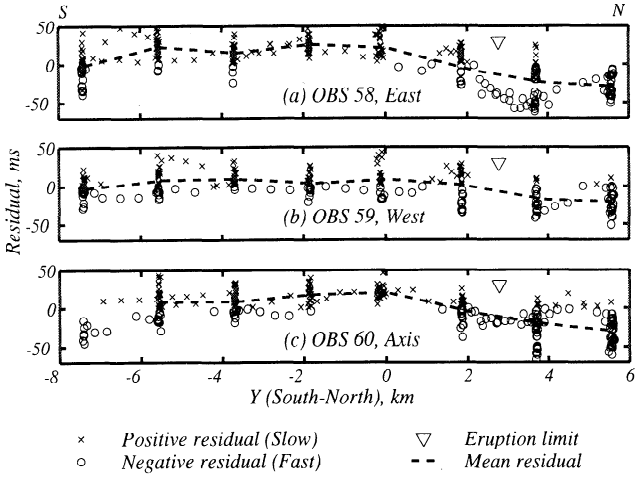

Figure 3. Travel time residuals (observed minus predicted) for the two-dimensional inversion of Figure 2 plotted as a function of the shot position along axis for (a) OBS 58 on the east flank, (b) OBS 59 on the west flank, and (c) OBS 60 on the ridge axis. Positive residuals (slow arrivals) are shown as crosses and negative residuals as open circles. Dashed lines connect the average residual for each across-axis shot line. An inverted triangle shows the northern limit of the 1991 eruption [*Haymon et al.*, 1993].

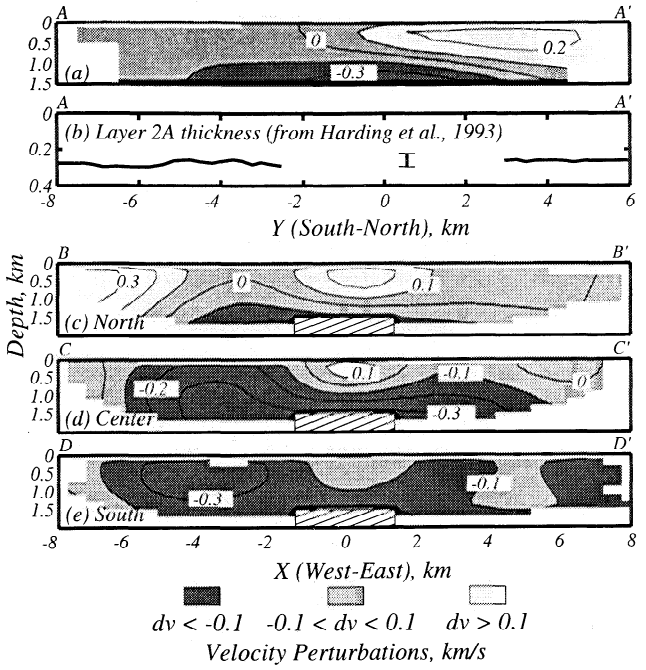

Figure 4. Results of a three dimensional inversion. (a) Velocity perturbations for a cross-section oriented along axis. (b) Axial layer 2A thicknesses calculated from the multichannel seismic data of Harding et al. [1993]. The solid lines are for an along-axis profile. The vertical bar shows the range of thicknesses observed within 0.5 km of the ridge axis along a cross-axis profile. (c-e) Velocity perturbations for three cross-sections oriented across the ridge axis. The location of the cross-sections is shown in Figure 1.

for shots to the north, there is a pronounced minimum for paths parallel to the ridge axis. Although our data set cannot discriminate unambiguously between anisotropy and fine scale heterogeneity, this pattern is consistent with an increase in fracture induced anisotropy to the north. To test this idea further, we obtained a series of two-dimensional inversions with fixed levels of anisotropy [*Barclay et al.*, 1998] for two data subsets comprising shots to the north and south of the OBS line. For the southern data subset, the minimum RMS residual and the least azimuthally dependent distribution of mean residuals is obtained with 2-3% anisotropy, while ~7% anisotropy is required for the northern subset.

The experiment geometry may allow a significant trade-off between anisotropy and three-dimensional structure. Thus, we inverted for three-dimensional models with fixed levels of anisotropy up to 8%. Although some features in the solutions are dependent on the level of anisotropy, all the solutions show a pronounced increase in velocities in the northern part of the experiment. Since the effect of increased levels of crack-induced anisotropy in the northern part of the experiment would be to decrease isotropic velocities, we infer that this northward increase in velocities is a robust result.

4. Discussion

The primary new result of our study is the detection of a pronounced decrease in average upper crustal velocities south of about 9°52'N both on and off axis. The observed change in velocity structure coincides with a fourth-order segment boundary at 9° 51.5'N which marks the northern limit of the 1991 eruption and of vigorous hydrothermalism [*Haymon et al.*, 1991, 1993]. Moving north across the boundary, the axial summit caldera narrows, the density of seafloor fractures increases, the lavas are older, and the dominant lava flow morphology changes from jumbled sheet flows to pillow basalts [*Haymon et al.*, 1991, 1993; *Perfit and Chadwick*, 1998].

The abrupt change in shallow crustal seismic structure detected near 9°52'N may arise from changes in the thickness of layer 2A or, alternatively, along axis variations in physical properties such as temperature, resulting from recent volcanism. Assuming a layer 2A velocity of 2.5 km/s, the average thickness of layer 2A would have to increase southward by nearly 100 m to explain our data. It is unlikely, however, that along axis changes in the axial velocity anomaly can be explained by variations in layer 2A thickness. Multi-channel seismic (MCS) data [*Harding et al*, 1993] reveal no significant change in on-axis layer 2A thickness across our study area (Figure 4b).

An alternative explanation for the along-axis variation in seismic velocities is a change in temperature within the sheeted dikes [*Toomey et al.*, 1994]. An along axis velocity contrast of 0.2-0.3 km/s implies an average thermal anomaly in the sheeted dike layer of at least 300°C [*Christensen*, 1979]. High levels of hydrothermal activity have persisted for at least a decade between 9°45' and 9°51.5'N, requiring a substantial heat source which is likely located in a thermal boundary layer above the AMC. In contrast the segment north of 9°51.5'N is hydrothermally inactive and the sheeted dikes may be relatively cold. The vertical resolution of our inversions is insufficient to constrain the thickness of the thermal boundary layer. A seismic cracking event observed at 9°50'N by *Sohn et al.* [1998] suggests that at one location elevated temperatures extend at least 300-600 m above the AMC. Near 9°30'N, *Toomey et al.* [1994] show that tomographic models are consistent with a 300- to 500-m-thick thermal anomaly above the AMC. Given the high intensity of

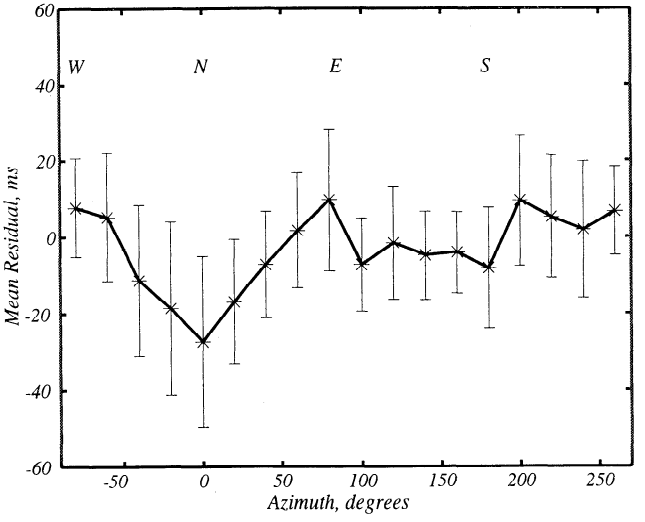

Figure 5. Travel-time residuals (observed minus predicted) for the three-dimensional inversion of Figure 4 averaged in 20° azimuth bins and plotted against the source-receiver azimuth. The azimuth is calculated relative to the orientation of the ridge axis. Error bars show the standard deviation of the residuals (not the standard deviation of the mean).

hydrothermalism at 9°45'-9°51.5'N and the history of recent volcanism, it is conceivable that thermal anomalies extend to shallower depths.

The results of *Toomey et al.* [1994] for 9°30'N show that the boundaries of a fourth-order segment are characterized by a decrease in the amplitude of a low-velocity anomaly above the AMC and an increase in the width of the near-surface axial high-velocity anomaly. In contrast to our experiment area, the segmentation at 9°30'N is not apparent in the upper crustal velocity structure off-axis. Although our tomographic models have much poorer resolution than those at 9°30'N, the magnitude of the along-axis change in travel-time residuals suggests that the 9°52'N segment boundary is characterized by a larger and longer-lived change in upper-crustal structure which has persisted for ~10^5 years.

Off-axis variations in shallow crustal seismic structure are probably not the result of temperature anomalies, since it is physically implausible that elevated temperatures persist far off-axis. Systematic along-axis variations in the basalt chemistry, the level of hydrothermal alteration, or the thickness of layer 2A could play a role. There is only one MCS profile crossing the rise axis in our study region [*Harding et al.*, 1993] and there are no independent observations which precludes ridge-parallel changes in off-axis layer 2A thickness. Although observations from the southern EPR show no general correlation between proxies for long-term magma supply and the thickness of off-axis layer 2A [*Hooft et al.*, 1997], such a relationship is not incompatible with models of crustal formation [*Hooft et al.*, 1996]. If a higher proportion of the eruption south of 9°51.5'N occur off-axis or are sufficiently voluminous to flow off-axis, layer 2A thickness could increase off-axis relative to the north without a corresponding change on axis.

Acknowledgments. We are grateful to the officers, crew, and scientific party of the R/V Maurice Ewing for assistance in carrying out the experiment. We thank Ken Creager and an anonymous reviewer for comments on an earlier draft. This work was supported by the National Science Foundation under grants OCE-9633814, OCE-9633264 and OCE-9634132.

References

Barclay, A. H., D. R. Toomey and S. C. Solomon, Seismic structure and crustal magmatism at the Mid-Atlantic Ridge, 35°N, *J. Geophys. Res., 103*, 17827-17844, 1998.

Barth, G. A., and J. C. Mutter, Variability in oceanic crustal thickness and structure: multichannel seismic reflection results from the northern East Pacific Rise, *J. Geophys. Res., 101*, 17951-17975, 1996.

Christensen, N. I., Compressional wave velocities in rocks at high temperatures and pressures, critical thermal gradients, and crustal low velocity zones, *J. Geophys. Res., 84*, 6849-6857, 1979.

Christeson, G. L., G. M. Purdy, and G.J. Fryer, Seismic constraints on shallow crustal emplacement processes at the fast spreading East Pacific Rise, *J. Geophys. Res.*, 99, 17957-17973, 1994.

Harding, A. J., G. M. Kent, and J. A. Orcutt, A multi-channel seismic investigation of upper crustal structure at 9°N on the East Pacific Rise, *J. Geophys. Res., 98*, 13,925-13,944, 1993.

Haymon, R. M., D. J. Fornari, M. H. Edwards, S. Carbotte, D. Wright, and K. C. Macdonald, Hydrothermal vent distribution along the East Pacific Rise crest (9°09'N-9°54'N) and its relationship to magmatic and tectonic processes on fast-spreading mid-ocean ridges, *Earth and Planet. Sci. Lett., 104*, 513-534, 1991.

Haymon, R. M., D. J. Fornari, K. L. Von Damm, M. D. Lilley, M. R. Perfit, J. M. Edmond, W. C. Shanks, R. A. Lutz, J. M. Grebmeier, S. Carbotte, D. Wright, E. McLaughlin, M. Smith, N. Beedle and E. Olson, Volcanic eruption of the mid-ocean ridge along the East Pacific Rise crest at 9°45-52'N: Direct submersible observations of seafloor phenomena associated with an eruption event in April, 1991, *Earth and Planet. Sci. Lett., 119*, 85-101, 1993.

Hooft, E. E. E., H. Schouten, and R. S. Detrick, Constraining crustal emplacement processes from the variation in seismic layer 2A thickness at the East Pacific Rise, *Earth and Planet. Sci. Lett., 142*, 289-309, 1996.

Hooft, E. E. E., R. S. Detrick, and G. M. Kent, Seismic structure and indicators of magma budget along the southern East Pacific Rise, *J. Geophys. Res., 102*, 27,319-27,340, 1997.

Moser, T. J., Shortest path calculation of seismic rays, *Geophysics, 56*, 59-67, 1991.

Perfit, M. R. and W. W. Chadwick, Jr., Magmatism at Mid-Ocean Ridges: constrains from volcanological and geochemical investigations, *in Faulting and Magmatism at Mid-Ocean Ridges*, edited by Buck, W. R., P. T. Delaney, J. A. Karson and T. Lagabrielle, pp. 59-115, *Amer. Geophys. Union Monogr., 106*, 1998.

Scheirer, D. S., and K. C. Macdonald, Variation in cross-sectional area of the axial ridge along the East Pacific Rise: evidence for the magmatic budget of a fast spreading center, *J. Geophys. Res., 98*, 7871-7885, 1993.

Sohn, R. A., D. J. Fornari, K. L. Von Damm, J. A. Hildebrand and S. C. Webb, Seismic and hydrothermal evidence for a cracking event on the East Pacific Rise crest at 9°50'N, *Nature, 396*, 159-161, 1998.

Toomey, D. R., G. M. Purdy, S. C. Solomon, and W. S .D. Wilcock, The three-dimensional seismic velocity structure of the East Pacific Rise near latitude 9°30'N, *Nature, 347*, 639-645, 1990.

Toomey, D. R., S. C. Solomon, and G. M. Purdy, Tomographic imaging of the shallow crustal structure of the East Pacific Rise at 9°30'N, *J. Geophys. Res., 99*, 24135-24157, 1994.

Toomey, D. R., W. S. D. Wilcock, R. S. Detrick and R. A. Dunn, Mapping melt and matrix flow in the uppermost mantle: preliminary results from undershooting the EPR (abstract), *Eos Trans. AGU, 79* (45), Fall Meeting Suppl., 805, 1998.

Vera, E. E., J. C. Mutter, P. Buhl, J. A. Orcutt, A. J. Harding, M. E. Kappus, R. S. Detrick and T. M. Brocher The structure of 0- to 0.2-m.y.-old oceanic crust at 9°N on the East Pacific Rise from expanded spread profiles, *J. Geophys. Res., 95*, 15529-15556, 1990.

Wilcock, W. S. D., S. C. Solomon, G. M. Purdy, and D. R. Toomey, Seismic attenuation structure of the East Pacific Rise near 9°30'N, *J. Geophys. Res.*, 100, 24147-24165, 1995.

R. S. Detrick, Department of Geology and Geophysics, Woods Hole Oceanographic Institutions, Woods Hole, MA 02543. (e-mail: rdetrick@whoi.edu)

T. Tian, Department of Electrical Engineering, Arizona State University, Tempe, AZ 85287 (e-mail: ttian@ocean.washington.edu)

D. R. Toomey, University of Oregon, 1272 Geological Sciences, Eugene, OR 97403 (e-mail: drt@newberry.uoregon.edu)

W. S. D. Wilcock, Box 357940, School of Oceanography, University of Washington, Seattle, WA 98195 (e-mail: wilcock@ocean.washington.edu)

(Received October 28, 1999; revised June 5, 2000;
accepted June 16, 2000.)